

RESEARCH ARTICLE | JUNE 27 2023

Crystallization in highly supersaturated, agitated sucrose solutions

Special Collection: [Special Issue on Food Physics](#)

Hannah M. Hartge   ; Eckhard Flöter  ; Thomas A. Vilgis  



Physics of Fluids 35, 064120 (2023)

<https://doi.org/10.1063/5.0150227>



View
Online



Export
Citation

[CrossMark](#)

Crystallization in highly supersaturated, agitated sucrose solutions

Cite as: Phys. Fluids **35**, 064120 (2023); doi: [10.1063/5.0150227](https://doi.org/10.1063/5.0150227)

Submitted: 13 March 2023 · Accepted: 11 May 2023 ·

Published Online: 27 June 2023



View Online



Export Citation



CrossMark

Hannah M. Hartge,^{1,2,a)}  Eckhard Flöter,²  and Thomas A. Vilgis^{1,a)} 

AFFILIATIONS

¹Max Planck Institute for Polymer Research, Ackermannweg 10, 55128 Mainz, Germany

²Chair of Food Process Engineering, Technische Universität Berlin, Straße des 17. Juni 135, 10623 Berlin, Germany

Note: This paper is part of the special topic, Special Issue on Food Physics.

^{a)}Authors to whom correspondence should be addressed: hartge@mpip-mainz.mpg.de and vilgis@mpip-mainz.mpg.de

ABSTRACT

Supersaturated sucrose solutions that have been sufficiently cooled without nucleation represent a metastable system in which agitation promotes fast crystallization. Applications of this physically interesting process can be found, for example, in the production of fondants in confectionery. This work considers supersaturated sucrose–water solutions under agitation, different temperatures, and concentrations as simplified fondant model systems. Although simple in composition, such solutions undergo complex kinetic and thermodynamic processes during crystallization under agitation. Main attention is paid to the torque during constant kneading of the samples at controlled temperature, accompanied by light microscopic examination of a characteristic sample. All torque curves show a characteristic minimum followed by a sharp peak during crystallization, which are attributed to an interplay of changes in concentration of the continuous liquid phase, formation of big conglomerates, and breaking of largest particles during continued growth. When comparing the crystallization times with classical nucleation theory, it is found that the variations are related to temperature and supersaturation in the same way as given by induction time models of thermodynamics and statistical physics.

© 2023 Author(s). All article content, except where otherwise noted, is licensed under a Creative Commons Attribution (CC BY) license (<http://creativecommons.org/licenses/by/4.0/>). <https://doi.org/10.1063/5.0150227>

I. INTRODUCTION

Fondants are sugar glazes or pastes often used in confectionery and pâtisserie that exhibit a unique mouthfeel. Their flow behavior, consistency, and texture are defined by a high fraction of sucrose crystals dispersed in a saturated sucrose solution.^{1,16,18} Fondant is produced by reducing hot sugar syrup to high concentrations of 80%–92% sucrose by weight, cooling while preventing preliminary crystallization, and then stirring the supersaturated system. The agitation induces rapid nucleation and crystal growth. Subsequently, crystals make up between 40% and 75% (w/w) of the final system depending on composition and temperature. Their sizes ideally range between 1 and 20 μm in diameter,^{1,2} and they can be regular or irregular in shape.

Fondant, thus, presents an intriguing and fascinating model system for studying crystallization and flow behavior, containing only sucrose and water as main components. However, fondant is hardly in the focus of scientific research in the field of physics. Although sucrose crystallization has been extensively studied in general and from various points of view,^{2–13} the specific conditions of high supersaturation, agitation, and a closed system introduce complicated processes and restrictions.

Many publications deal with crystal growth of sucrose, for example, in industrial crystallizers, discussing effects of supersaturation and agitation to some extent.^{12–15} However, mostly, the reported crystallization kinetics are solely valid for a small concentration range and single technical system, and applied research often focuses on crystallization with intentional seeding instead of homogeneous nucleation. Additionally, these studies usually relate to the subject in an applied, technical manner rather than from a basic physics perspective.

The sparse literature on fondants mainly discusses the effects of composition and preparation conditions on the final crystal quantity, size distribution, or shelf life.^{1,16–19} Here, the fondant systems studied usually contain additional components like glucose syrup, other sugars or sugar alcohols, and acidic ingredients or enzymes. Except for rather general statements or very narrow empirical data on crystallization rates¹⁶ within these condition ranges, there is little focus on understanding the underlying processes during crystallization.

Despite its simple basic compositions, the physics of fondant remains unclear. The reasons are manifold. The initial supersaturated solutions are metastable. Also their crystallization occurs under controlled cooling with simultaneous shearing with high shear forces,

therefore, under conditions far from equilibrium. To better understand the formation and physical behavior of fondant, it is inevitable to consider well-defined model systems, where physical parameters can be controlled. This approach makes it possible to better separate the temperature- and shear-induced processes and, thus, to better quantify the flow behavior of the fondant.

In general, solutions that are supersaturated constitute labile or metastable systems when at rest. Classical nucleation theory (CNT) predicts how temperature and supersaturation drive nucleation rates in such solutions exponentially. However, at very high concentrations, the low mobility and diffusivity of sucrose molecules hinder crystallization. This is especially true near the glass transition, when molecular mobility is very low, and this despite the fact that supersaturation is a strongly pronounced main driving force for crystallization. When such a system is agitated, the kinetic (or shear) energy supplied leads to rapid nucleation and crystal growth, with time scales much smaller than at rest in the supersaturated state.^{2,20–25}

Classical nucleation theory and its limitations are often cited in the literature on sucrose and confectionery,^{2,8,16,17} yet there is no study on whether it yields a meaningful approach to describing the process of fondant making. The present work aims to fill this gap and develop a better understanding of the general processes involved in sucrose crystal formation.

In the first part of this study, a qualitative examination and discussion of the torque curves during crystallization of different samples is presented. A typical experiment is presented in Fig. 1.

In combination with light microscopy images taken at different times of the process, it is concluded that (a) a drop in sucrose concentration within the liquid phase causes a drop in measured torque, (b) a high number of crystal conglomerates are formed initially, and that (c) these conglomerates mostly break apart during further kneading while smaller crystals still grow, leading to a peak and subsequent drop in torque. In the second part, the differences in crystallization times taken from the torque curves are compared with classical nucleation theory, showing good agreement. This allows to develop a better understanding of the composition and temperature dependency of the nucleation process.

II. THEORETICAL BACKGROUND: CLASSICAL NUCLEATION THEORY

For the first instance, it is sufficient to employ the classical nucleation theory. In this well-known, admittedly simple theory, the change in free energy of the molecules assembling in a crystal lattice is approximated compared to the molecules in solution and then related to an induction time implied by this energy change. The following derivation can be found in different text books on crystallization or literature on sucrose crystal formation, see, for example, Mullin²¹ (Chap. V), Markov,²² Vaccari and Mantovani,²⁰ or De Yoreo and Vekilov.²⁴

The change in free energy is mainly determined by the sum of two contributions: one accounting for the change in chemical potential for all the molecules that assemble in a lattice and the other for the change in interfacial energy.

While spheres are often used as a simple example in classical nucleation theory, for sucrose crystals, the nuclei will here be approximated more realistically by cubes with edge length l . This obviously is still a simplification, especially since shapes of nuclei often differ from equilibrium bulk crystal shapes, as De Yoreo and Vekilov point out²⁴ (pp. 68–71). Nonetheless, it gives a first approximation, and will only differ by a prefactor in the end (see also Sec. IV C for more details). So if nuclei are assumed to be cubic, the free energy change Δg can be written as the sum of a bulk and surface term as follows:

$$\Delta g = \Delta g_{\text{bulk}} + \Delta g_{\text{surf}}, \tag{1}$$

$$= -\frac{l^3}{\Omega} \Delta \mu + 6l^2 \alpha, \tag{2}$$

where, Ω is the volume of one sucrose molecule, $\Delta \mu$ is the difference in chemical potential between sucrose molecules in the supersaturated solution and sucrose molecules in equilibrium solution, and α denotes the interfacial free energy of the sucrose crystal lattice in solution per unit area.

Since the second term of Eq. (2) grows with l^2 , but the absolute value of the first, negative term grows faster with l^3 after smaller initial values, a maximum in the sum of both terms arises if taken with respect to the edge length l . This is illustrated in Fig. 2.

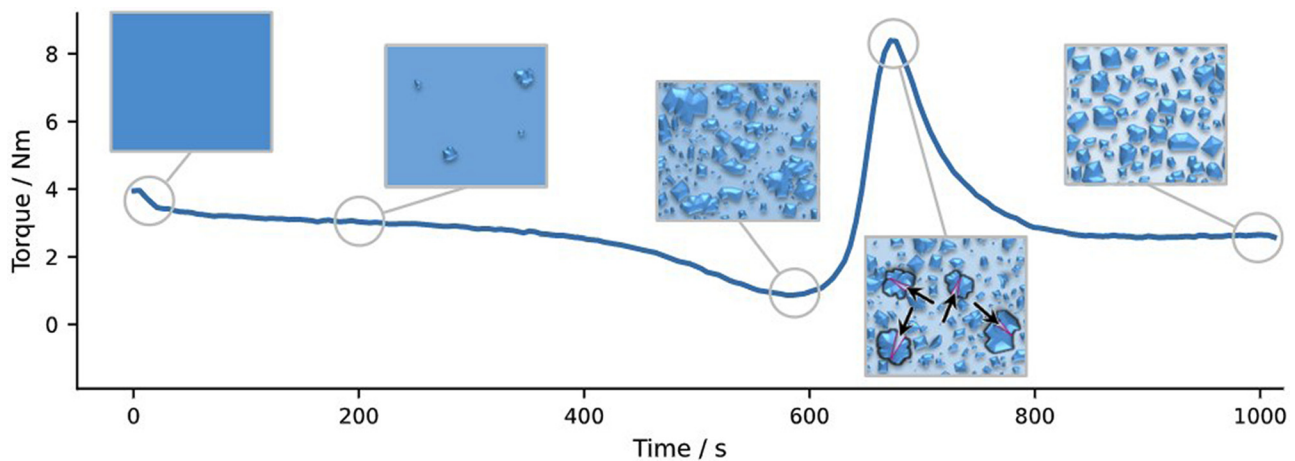


FIG. 1. Averaged torque curve during the kneading process of a solution with 85% (w/w) sucrose, with sketches of the corresponding stages in the crystallization process.

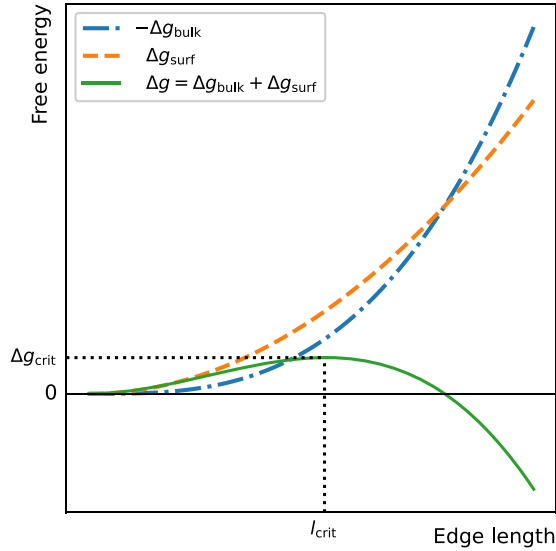


FIG. 2. Absolute value of the bulk term of free energy rises slower with nucleus edge length than the surface term; Δg_{bulk} is depicted in negative here for better visualization. The sum of bulk and surface term in free energy change Δg shows a maximum, resulting in an energy barrier overcome at a critical edge length of the nucleus.

The maximum in $\Delta g(l)$ resembles the critical edge length l_{crit} that a nucleus has to exceed in order to overcome the energy barrier of interfacial free energy and remain stable. This is because for $l > l_{\text{crit}}$, the slope of Δg becomes negative and, thus, keeps the nuclei from disassembling again by mere statistical processes (see Fig. 2). This critical edge length can be calculated by deriving the free energy term Δg by l and setting it equal to zero.

The chemical potential of solutes in solutions depends primarily on the concentration of the solute, which must be above the saturation concentration for nucleation to be possible. Chemical potentials are usually expressed via its chemical activity a , its chemical potential at a reference state μ_0 , and with respect to Temperature T and Boltzmann constant k_B as $\mu = \mu_0 + k_B T \ln(a)$. Thus, the difference in chemical potential can be given as $\Delta\mu = \mu - \mu_{\text{sat}} = k_B T \ln(a/a_{\text{sat}})$. Introducing supersaturation defined as $\beta = a/a_{\text{sat}}$ (see also Sec. IV C for a discussion), for the critical edge length l_{crit} ,

$$\frac{d\Delta g}{dl} = 0 \Rightarrow l_{\text{crit}} = \frac{4\Omega\alpha}{\Delta\mu} = \frac{4\Omega\alpha}{k_B T \ln(\beta)}. \quad (3)$$

With this expression for l_{crit} , the change in free energy that is found for a nucleus exactly at the size of the critical edge length Δg_{crit} can be expressed as

$$\Delta g_{\text{crit}} = 32\alpha^3 \left(\frac{\Omega}{k_B T \ln(\beta)} \right)^2 \propto \frac{1}{T^2 (\ln \beta)^2}. \quad (4)$$

Now, with help of the Arrhenius reaction rate equation, the rate of nucleation J_{nuc} can be estimated as proportional to the exponential of its change in free energy divided by $k_B T$. This gives the predicted rate of nucleation events as follows:

$$J_{\text{nuc}} = \tilde{A} \exp\left(-\frac{\Delta g_{\text{crit}}}{k_B T}\right), \quad (5)$$

where, \tilde{A} is a prefactor depending on many variables that accounts for the number of molecules meeting possible nucleation sites and for probability of adsorption. Thus, an expression for the induction time τ of nucleation, which is defined as the reciprocal of J_{nuc} , can be written as follows:

$$\tau = \frac{1}{J_{\text{nuc}}} = A \exp\left(\frac{32\Omega^2\alpha^3}{(k_B T)^3 (\ln \beta)^2}\right), \quad (6)$$

where $A = 1/\tilde{A}$.

From this, it can be seen that the induction time for nucleation statistically depends on the temperature cubed, and on (logarithm of) supersaturation squared, both decreasing induction time dramatically when rising. This approximation has its limitations in practice, of course, which are discussed in more detail in Sec. IV C. Nevertheless, some new insights for fondants can be formulated.

III. MATERIALS AND METHODS

A. Chemicals

Sucrose was provided as crystalline white sugar (extra fine) by Südzucker AG (Mannheim, Germany). Water was filtered and deionized using a Milli-Q[®] water purification system.

B. Sample preparation

To prepare supersaturated sucrose solutions, 20% of water was combined with 80% sucrose by weight for all samples. Thus, complete dissolution of sucrose could be achieved before boiling down to the desired final concentration. The total amount was calculated such that the sample would yield about 325 ml of solution after evaporating enough water to reach the chosen target concentration (see the supplementary material for more details). This volume was chosen in order to meet the 300 ml of maximum volume given by the kneading device while accounting for the loss observed during transfer of the sample.

Sucrose and water were placed in a pot together with a magnetic stirrer, covered with aluminum foil and put on a heating plate, with a mixing speed of 100 rpm and heating temperature of 100 °C at the beginning. As soon as the stirrer moved freely in the mixture, usually at a sample temperature of (70 ± 5) °C, heating temperature was increased to 300 °C to allow for a quick heating process. The cover was removed, and stirring was stopped when the syrup was clear and no more crystals were visible; this was obtained at a sample temperature of (110 ± 2) °C. The mixture was then boiled down and repeatedly weighted on a scale until the desired sucrose concentration of 80%, 82.5%, 85%, 87.5%, or 90% (w/w) was reached. Final sample temperatures were between 110 °C (80% sucrose) and 120 °C (90% sucrose).

The syrup was poured into a deep dish of 28×28 cm² to allow for initial quick cooling and, thus, inhibit prior crystallization. It was then placed into a water bath at a temperature depending on the aimed kneading temperature. When the solution reached a temperature of about 5 °C above kneading temperature, the syrup was scraped into the preheated measuring kneader.



FIG. 3. Measuring kneader used for agitation and measuring torque. Showing open trough with inserted thermometer.

C. Crystallization and torque measurement

Agitation was conducted in an IKAVISC Measuring Kneader MKD 0.6-H60 (IKA Werke GmbH & Co. KG, Staufen, Germany) for high viscosity samples (see Fig. 3). Data were collected via an in-house datalogger and own software. Preheating was achieved via water circulation in such a way that inside of the trough a chosen temperature of 25 or 44 °C was reached. The kneader was started at its maximum speed of 67 ± 1 rpm (verified via calibration by eye and timer), and data of speed, temperature, and torque were collected. As soon as the torque showed a characteristic peak indicating rapid crystallization of the sample, tempering water was switched to room temperature to cool down the sample. This was done in order to let all samples cool down rather homogeneously before further analysis. If not stated otherwise, kneading time was adjusted individually for each sample and in such a way that total kneading time was $t_{\text{tot}} = 1.5t_p$, with t_p being the time until the torque peak maximum was observed.

Each torque measurement was performed in triplicate. For further calculations, the individual torque curves were first smoothed using a Savitzky–Golay filter (window length 15, second order polynomial). Afterward, average and standard deviation of the peak time for each parameter combination were calculated and plotted via Python.

D. Light microscopy

For analysis of crystal formation during the kneading process of a characteristic sample, a preparation containing 85% (w/w) sucrose kneaded at 25 °C was chosen for further observation via microscopy. Agitation of the sample was stopped at $t = 200$ s, $t = 400$ s, at the torque minimum t_{min} , at the peak time t_p , and after the full process t_{tot} . Samples were then instantly prepared for microscopy.

To allow for observing individual crystals and to quickly slow down crystallization, the crystallized sample was immediately diluted with pre-tempered, saturated sucrose solution (25 °C). This solution was prepared by mixing 70 g sucrose with 30 g distilled water in a glass beaker covered with Parafilm® at 400 rpm overnight, then centrifuging the syrup at 15 000 g for 10 min at 25 °C. The sucrose sedimented to the bottom was left inside the centrifuge tubes to ensure continuous saturation, and saturated solution was only taken from the top. The fondant sample was then mixed with saturated solution by hand with a flexible, disposable spatula and pipetted onto a glass slide, then gently covered and distributed with a cover glass. Eight images were taken with a digital camera mounted onto a Zeiss AxioScope.A1 (Carl Zeiss AG, Oberkochen, Germany) in bright field transmission mode at 20× magnification. At least four microscopy images per sample were taken for particle characterization.

IV. RESULTS AND DISCUSSION

The averaged torque curves of samples with 80%–90% (w/w) sucrose concentration agitated in the measuring kneader at 25 °C or 44 °C are depicted in Fig. 4. Comparing these curves, a characteristic pattern can be observed: Although the beginning of the process mostly shows a plateau, slight rise or even slow decrease in the torque (indicating necessary time for homogeneous distribution of the sample within the trough), each measurement then shows a notable decrease in the torque with subsequent sharp peak afterward.

The peak is the most prominent feature of these curves and arises when a large part of sucrose is crystallized; details of the process are

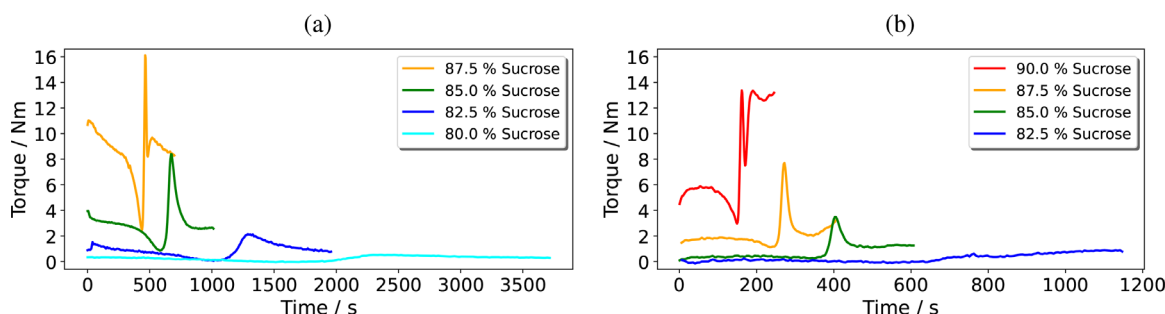


FIG. 4. Averaged, smoothed torque curves of samples with varying concentration kneaded at (a) 25 °C and (b) 44 °C. Sucrose content in weight percent. Note the stretched timescale in the right plot.

discussed below. When comparing the different samples at the same temperature, the peak flattens with lower sucrose content. This is to be expected due to a larger liquid fraction and thus lower viscosity of the dispersion. Also, peaks are shifted to longer times. Comparison of samples agitated at 25 °C and at 44 °C shows again smaller peak maxima at elevated temperature. Again, this can be explained by higher sucrose solubility and, thus, a lower fraction of crystallized sucrose, but also due to lower viscosity of the liquid phase. Times until the peak occurs are significantly reduced for higher temperature.

In the following, the question of the cause of the torque minimum will be considered first, and why afterward the torque rises to a prominent maximum with subsequent decrease.

A. Decrease in torque before peak

Since highly concentrated, coarse poly-disperse systems like fondant propose a difficult challenge for theoretical models of flow, we will mainly stress qualitative relations here. According to semi-empirical models of dispersion viscosities, one finds viscosity η to be increasing with the volume fraction of dispersed particles Φ ²⁶ (see Appendix A for more details on such models). This dependency is strong, often in the form of a power law, and viscosity tends toward infinity when approaching maximum possible packing density.²⁶ This effect is visualized in Fig. 5(a).

Therefore, when the sucrose starts to crystallize induced by agitation, at first sight, a rise in apparent viscosity—and thus, in measured torque—could be expected due to an increase in the volume fraction and size of solid particles within the dispersion. The observed decrease in measured torque, even though limited, thus, might seem counter intuitive.

A first explanation of these observations is to argue that temperature rises within the sample due to heat released during crystallization and due to friction within the solution/suspension. Indeed, a slight increase in temperature can be measured inside the kneading trough until the torque minimum is reached, despite the cooling water. Since viscosity of such supersaturated sucrose solutions is strongly dependent on temperature,^{8,27,28} it is to be expected that temperature changes lead to measurable effects in the torque. This observed temperature increase is measured to be about roughly 2 °C in the inside of the kneading cell, and can be assumed to be even less closer to the walls, where the solution is most effectively cooled by the water circulation system and contributes most to measured torque.

The torque is measured to drop by roughly 75% of its starting value for all 25 °C samples. In the graphs of Fig. 4(a), this can, for example, be seen for the sample containing 85% sucrose: Here, the

torque decreases from about 3.3 N m to about 0.86 N m. Looking at literature data²⁹ (see Appendix B for details), a solution containing 85% (w/w) dissolved sucrose shows a viscosity of about 237 Pa s at 25 °C, and a decrease to about 172 Pa s is to be expected for a temperature rise by 2 °C. This yields a decrease in viscosity by about 27%, so much less than the observed 74%. Even if an error in temperature measurement is assumed and a temperature rise by 5 °C is considered, this should lead to a decrease by about 54%, still significantly less than the observed amount. Changes in temperature, thus, cannot solely account for the dramatic decrease in torque.

Microscopy images taken of a sample with 85% (w/w) sucrose kneaded at 25 °C after 200 s, 400 s, and at the minimum clearly show that crystallization has already started at 200 s to a small extent, and a major crystalline fraction was present at the time of the torque minimum. Images of every stage can be found in the supplementary material of this article.

Thus, next to changes in temperature, two additional processes have to be taken into account when looking at the apparent viscosity during agitation: First, there is an increase in volume fraction of solid particles, starting from zero and rising monotonically until all excess sucrose is crystallized out of solution. Second, when nucleation and initial growth of small crystallites is enabled, this leads to an accumulation of sucrose molecules in discrete areas. By that the sucrose concentration of the continuous liquid phase is decreased locally with every sucrose molecule that is assembled in a crystal lattice. This in turn decreases its viscosity. This dependency is visualized in Fig. 5(b).

Thus, a measurable decrease in viscosity of the liquid phase during nucleation is inevitable, which at this point still makes up most of the dispersion’s volume, with hard particles being scattered and rarely touching in the beginning. If, for example, the point is considered where the concentration of dissolved sucrose has reduced from 85% to about 83%, the suspension will only contain a little more than $\Phi = 1.8\%$ particles by volume. At the same time, empirical values yield a drop in viscosity from 237 Pa s to just 59 Pa s in the continuous liquid phase due to the reduction in concentration.^{28,29} The overall apparent viscosity is, thus, mainly dependent on the thinning syrup at this first stage.

An estimate of the lower limit of viscosity in the immediate vicinity of nuclei is provided by the viscosity of a solution with equilibrium saturation at the same temperature: For 25 °C, this is given by a solution of about 67.47% (w/w)^{28,30} sucrose, yielding 0.18 Pa s (again, see Appendix B for details on the determination of these values). Considering the slight temperature increase to 27 °C, the equilibrium solution would contain 67.79% (w/w) sucrose with a viscosity of

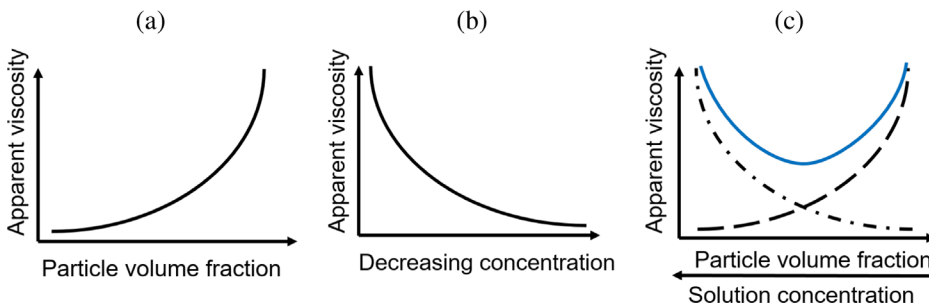


FIG. 5. Sketches of viscosity changes during crystallization out of homogeneous solution, visualizing (a) rise of viscosity with rising particle volume fraction, (b) decrease in viscosity with decreasing solution concentration, and (c) occurrence of a minimum with concurrent changes in particle volume fraction and solution concentration.

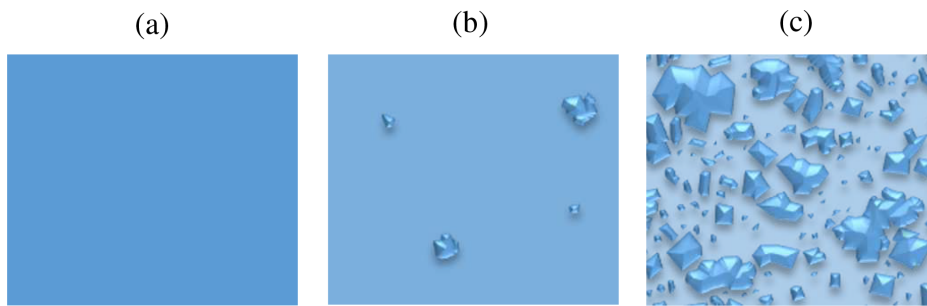


FIG. 6. Sketches based on microscopy images of the crystallization process out of homogeneous solution (a) at the beginning of the process, (b) after 200 s, and (c) at the minimum in measured torque.

0.16 Pa s. Consequently, a viscosity drop in the continuous phase of three orders of magnitude is to be expected over the entire course of crystallization.

Thus, the different processes at hand have counteracting effects on overall apparent viscosity of the suspension, as is also suggested by Hartel² for a similar observation (based on a Master’s thesis by Shastry,³¹ as cited in Hartel,² p. 73).

At appropriate times, the increasing crystal volume fraction exceeds a value at which the particles start interfering when sheared, with too little fluid left to separate them from each other. Friction between the growing hard crystals then rises faster than the dropping

solution concentration decreases viscosity at some point. This in turn leads the measured torque to increase again. The overlapping of the two effects leads to a minimum in apparent viscosity of the suspension during crystallization and, thus, to a minimum in measured torque. This is roughly sketched in Fig. 5(c).

Sketched visualizations of crystallization at all three stages—first a homogeneous solution, then a decrease in concentration in the continuous liquid phase during nucleation and first crystal growth, last the rise in particle interaction and friction due to increasing crystal size—is shown in Fig. 6 at microscopic scale.

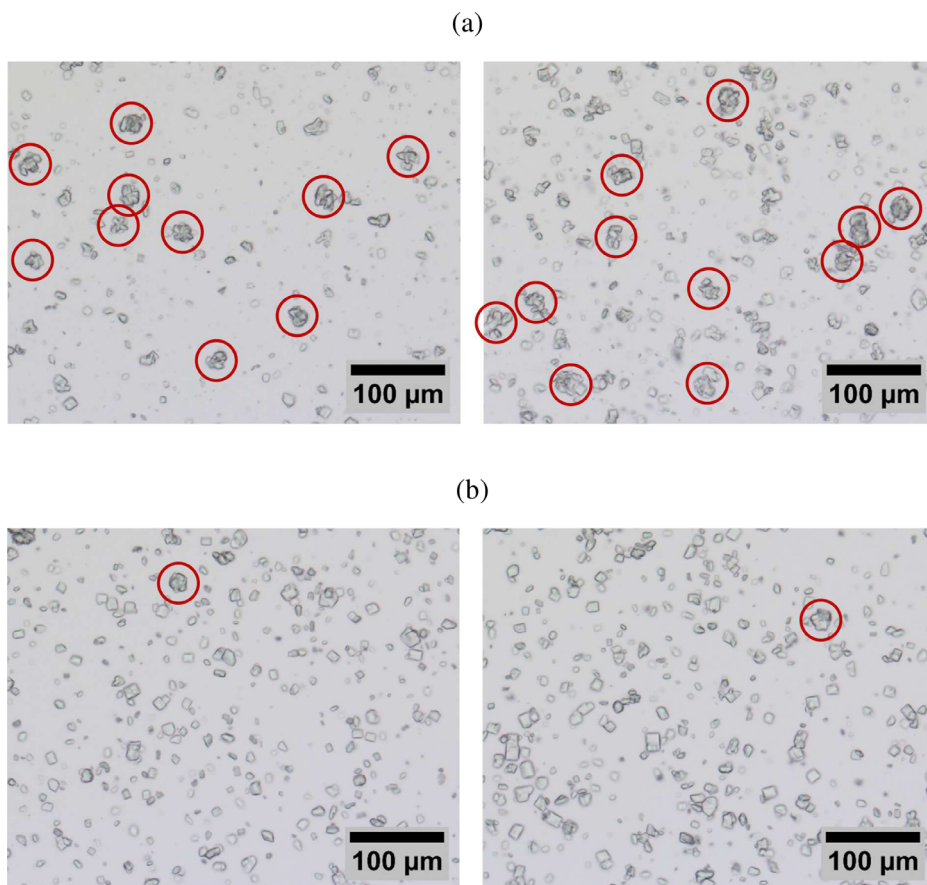


FIG. 7. Typical microscopy images of samples containing 85% (w/w) sucrose, kneaded at 25 °C until (a) the torque peak occurred and (b) the full process. Diluted with saturated sucrose syrup by about 1:25. Red circles placed around some visible conglomerates in each case.

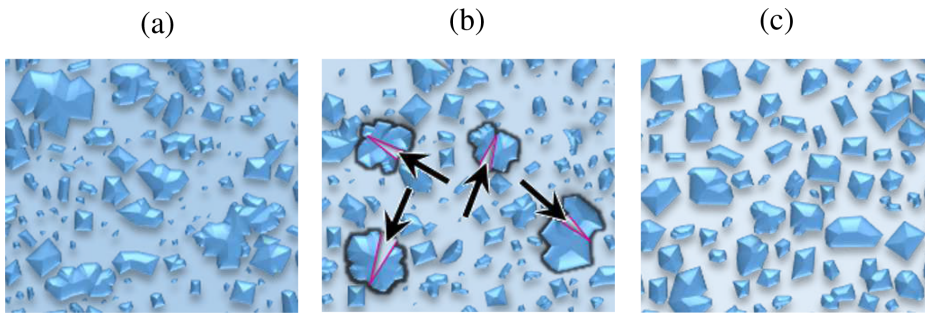


FIG. 8. Steps of the crystallization process under agitation (a) at the torque minimum, (b) at the torque peak, and (c) at the end of the process.

It is important to point out here that the exact behavior of the apparent viscosity and the measured torque depends strongly on the geometry of the stirring motion. In the case of this setting, it not only induces shear but, in some parts, also simultaneous compression in a confined space (see Fig. 3), which prevents crystals from orientating in a way to minimize friction.

B. Decrease in torque after peak

While the rise in the torque can easily be referred to the growing crystals and rising friction as discussed above, the formation of a maximum and sudden fall of measured torque needs further explanation. To get a better picture of what is happening here, images of a sample with 85% (w/w) sucrose were taken via light microscopy. Figure 7(a) shows the sample after stopping the kneading process as soon as the peak occurred (about 11 min after start of agitation) and after dilution with saturated syrup (see the supplementary material for more details).

Light microscopy of such samples shows a high number of crystal conglomerates. This observation can be explained by the high supersaturation levels at hand, which are known to promote formation of such conglomerates.²⁰ Also agitation supports crystals to grow together when growing in close proximity and hitting each other due to shearing. Together with secondary nucleation—the formation of nuclei on preexisting solid material (see Mullin,²¹ Chap. 5.2)—this can lead to numerous crystal conglomerates intraconnected by sub-optimal lattice sites. If compared to images of samples with the same

composition, but kneaded full time (1.5 times as long as it takes for the peak to occur), one can mainly observe two differences: For the latter, as shown in Fig. 7(b), the number of larger conglomerates seems to have been reduced drastically (although not completely vanished), while at the same time, the smallest particles have also increased in size or vanished.

In sum, the overall size distribution is narrowing down around a smaller median diameter (weighted by area). The overall process is visualized in Fig. 8.

Thus, it is indicated that the kneading and resulting friction among the growing crystals leads to shear forces high enough to break down large conglomerates, while small particles and broken fractions are still growing. The breaking of conglomerates seems to be expected in particular, because such conglomerates have weak sites at their junction zones.^{20,32} The continuation of the growth process is indicated by the observation of more regularly shaped crystals at the end of the process: Smaller particles or fragments seem to either dissolve again^{21,25,33} or grow and develop more regular faces over time. This can be explained by the fact that in the later stages of the process, supersaturation in the liquid face becomes smaller and smaller, reducing pressure on crystal growth and, thus, allowing for more regular crystals.

C. Time dependency of torque peak

When comparing different samples varying in composition and crystallization temperature, the most prominent difference is the length of time that elapses before substantial crystallization is reached.

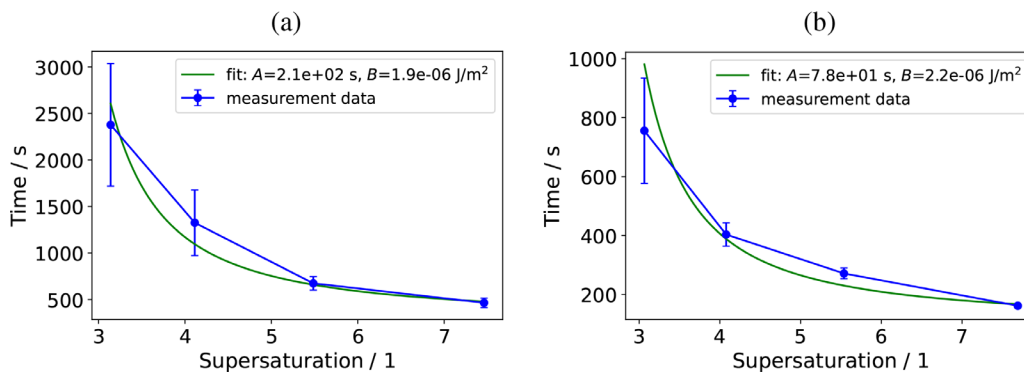


FIG. 9. Agitation time until peak in measured torque (blue dots) occurs with respect to calculated supersaturation, conducted at (a) 25 °C and (b) 44 °C, and fit according to Eq. (9) (green line). Error bars on time axis represent standard deviation of the measurements.

24 July 2023 10:21:23

These differences in time lengths are compared in the following section and their values depending on different compositions, as can be seen in Fig. 9.

The maxima of the torque were chosen for comparison, although the exact occurrence of each maximum is dependent on a combination of different factors.

For example, before stable nuclei are formed, sucrose molecules cluster together and other molecules stack around them, with many of these clusters never reaching the critical size. After formation of stable nuclei, which is treated here via classical nucleation theory, crystal growth is described to be determined by different steps (see Mathlouthi and Genotelle¹⁰ for a discussion): diffusion from the bulk solution to the crystals surface, desolvation, molecular alignment, and incorporation of sucrose molecules into the crystal lattice.

So, of course, the onset of nucleation takes place much earlier (as also results from Sec. IV A) than the torque peak, and, hence, would be more indicative of the underlying fundamental processes. This onset can hardly be determined from the torque data curves though. The peak maximum was found to be the only feature that was reliably and precisely determinable from datasets.

While many different factors contribute to the occurrence of the peak maximum—start and rate of nucleation, crystal growth speed, amount of sucrose to crystallize, size and number limit for crystals to start breaking due to friction—it is reasonable to assume that nucleation is the main contributor to timescale. This is mainly because nucleation depends dramatically on supersaturation [see Eq. (6)], while the dependence of crystal growth on supersaturation is significantly lower.¹⁰ Thus, t_p is taken as an indicator for induction time of nucleation.

With regard to the thermodynamic approach of classical nucleation theory presented in Sec. II, limits of the simplistic Eq. (6) have to be taken into account. With supersaturation approaching very high values, molecule diffusivity is reduced considerably, which leads to a decreased nucleation rate and higher induction times. For example, an aqueous solution containing about 90% (w/w) sucrose is measured to show a sucrose diffusion coefficient on the order of $10^{-18} \text{ m}^2 \text{ s}^{-1}$ at room temperature, opposed to $10^{-12} \text{ m}^2 \text{ s}^{-1}$ for a solution containing about 70% (w/w) sucrose.³⁴ In viscous systems like highly supersaturated sucrose solutions, this diffusion barrier increases induction times to the order of hours or days in quiescent conditions as they approach the glass transition temperature, where they would crystallize rapidly if governed by supersaturation alone.^{2,8,35}

Nevertheless, the supersaturated solutions considered here stay above the glass transition.³⁴ Champion *et al.*³⁶ extrapolated with a series of experiments with sucrose solutions in different concentrations translation diffusion constants on the order of magnitude $D_{T_g} \sim 10^{-24} \text{ m}^2/\text{s}$ at the glass transition temperature T_g . Using these extrapolation results,³⁶ $T_g/T \simeq 0.86$, the glass transition temperature estimates $T_g \sim -16^\circ \text{C}$ according to the mastercurve [similar to T_g for 90% (w/w) sucrose solutions according to the Gordon–Taylor equation in Ref. 36].

Additionally, in the cases studied here, two simultaneously competing effects take place: collision of crystals during shearing and the change in the glass transition temperature³⁷ by (re-)crystallization. Both influence crystallization in different ways. The former by breaking off of crystal fragments of which many dissolve again and increase liquid concentration, yet others serve as new nuclei, while the collision kinetic is mainly controlled by agitation speed²⁵ (which is constant in

all measurements). The latter by changes in diffusivity following the changes in liquid concentration.³⁴ These complex counteracting processes make a precise prediction of nucleation times unachievable, but the comparison with the basic relations of classical nucleation theory still provide better understanding of the dominant underlying thermodynamic processes.

In this work, agitation speed is kept at a constant level of roughly one revolution per second for all measurements. With a typical radius in the kneader of about 3 cm, this equals a velocity on the order of 10^{-1} m s^{-1} . Thus, the time and length scales of the agitation are by several orders of magnitudes smaller compared to the molecular time scales. Consequently, their influence can be matched in a constant prefactor, since the time scales are clearly separated in contrast to the cases considered, for example, by Mura and Zaccone³⁸ or Richard and Speck.³⁹

Another aspect to be considered is the type of nucleation at hand: The relation described in Eq. (6) is depending on the assumption that nucleation is homogeneous, with nuclei forming in the pure homogeneous liquid and growing to a cubic shape. Crystal formation with the starting point at a foreign surface though, known as heterogeneous nucleation, is far more prevalent in practice. This can happen where the supersaturated liquid touches walls of a container or air, or when impurities such as dust are present in the liquid.

Classical nucleation theory predicts that heterogeneous nucleation can even take place when the probability of homogeneous nucleation is practically negligible, as is also the case empirically. (See also, e.g., Mullin²¹ and Markov²² for a more detailed discussion of heterogeneous nucleation, which is summarized here according to the present purpose.) Because nuclei on surfaces are not fully immersed, reducing the contact area of nucleus and liquid, the energy barrier created by surface formation is reduced and, thus, nucleation rate is increased. This of course only is true if the interfacial energy between crystal nucleus and third surface is lower than that between nucleus and solution. This is often the case, especially with solid contaminants on container walls, since molecules in the crystal can form stronger bonds with molecules in the solid than with those in solution.

For Δg in Eq. (2), this will result in a modified term of surface size and interfacial free energy α . Assuming a cubic nucleus growing on a foreign substrate with one of its six faces, Δg_{surf} will become $l^2(5\alpha_{\text{cl}} + \alpha_{\text{cs}} - \alpha_{\text{sl}})$ with subscripts “cl” denoting crystal–liquid, “cs” crystal–substrate, and “sl” substrate–liquid interface. The critical nucleus length then becomes $l_{\text{crit}} = -\Omega/(3\Delta\mu)(5\alpha_{\text{cl}} + \alpha_{\text{cs}} - \alpha_{\text{sl}})$, and the energy barrier to overcome for a stable nucleus is

$$\Delta g_{\text{crit}} = \frac{20}{27} \left(\frac{\Omega}{\Delta\mu} \right)^2 (5\alpha_{\text{cl}} + \alpha_{\text{cs}} - \alpha_{\text{sl}})^3 \quad (7)$$

$$= B \left(\frac{\Omega}{k_B T \ln(\beta)} \right)^2, \quad (8)$$

where the factor B contains the specific values of surface size, shape, and interfacial free energies. Accounting for different angles between crystal and foreign substrate, for example, at uneven or scratched surfaces, would change the prefactor B accordingly. Equation (6) then can be generalized to

$$\tau = A \exp \left(B \frac{\Omega^2}{(k_B T)^3 (\ln \beta)^2} \right). \quad (9)$$

To calculate nucleation times, supersaturation $\beta = a/a_{\text{sat}} = \exp(\Delta\mu/k_B T)$ is a crucial thermodynamic parameter, yet hardly measurable in practice. Therefore, β is usually approximated by making use of the given concentration and equilibrium saturation.

More precisely, supersaturation should be calculated as $\beta = a/a_{\text{sat}} = (\gamma x)/(\gamma_{\text{sat}} x_{\text{sat}})$ by definition, with γ being the activity coefficient of solute at the given state and x being the mole fraction of the solute.⁴⁰ (Note that Schall *et al.* use a different definition of β including the logarithm,⁴⁰ which is merely a matter of different convention if the logarithm is included in the equation for Δg in one way or the other.) Activity coefficients are often neglected in approximation of sucrose supersaturation,^{7,12} although, especially at high concentrations, they will considerably alter values of β .

In this study, a modified molecular UNIQUAC model for estimation of activity coefficients is used. This quasichemical model was successfully applied to sucrose and other sugars for a wide range of concentrations by Peres and Macedo,⁴¹ and, thus, their calculated parameters are adopted in this work, as also seen, for example, in Ouiazzane *et al.*¹² The resulting equation yields values for $\gamma(x, T)$ and $\gamma_{\text{sat}}(x_{\text{sat}}, T)$ (see Appendix C for details).

As before in Sec. IV A, values for equilibrium saturations at the given temperatures were calculated according to Bubnik and Kadlec³⁰/ICUMSA²⁸ (see Appendix B). This gives about 67.47% (w/w) for 25 °C, equaling $x_{\text{sat}} \approx 0.098$, and about 70.89% (w/w) for 44 °C, equaling $x_{\text{sat}} \approx 0.114$. $\beta = (\gamma x)/(\gamma_{\text{sat}} x_{\text{sat}})$ was calculated using these values in order to model measured peak times of all experiments with respect to temperature and supersaturation. The data points for peak times t were, thus, fitted according to Eq. (9) with A and B set as fitting parameters. The resulting fit curves are shown in Fig. 9.

The fitted curves match the data points quite well, with the fitting factor B taking a value of 1.9 and $2.2 \times 10^{-6} \text{ J m}^{-2}$, respectively. Considering the simplicity of the underlying model and the complexity of the processes, this shows the proposed thermodynamic approach to be in good accordance with experimental results. Here, as already discussed, the fitting parameters A and B have to take account for changes in the free energy term due to agitation and heterogeneous nucleation, crystal growth speed, and time until the sucrose crystals break faster due to friction than they grow. Hence, it is not attempted here to give precise physical meaning to these fitting parameters, but we argue that even with this simple approach, we can show the viscosity peak time is related to temperature and supersaturation in a way to be theoretically expected for induction time $\tau(T, \beta)$ by thermodynamic models. This in turn indicates a direct relation between measured peak time and statistical induction time for nucleation, and that the proposed model represents a good approach to understanding the main physical processes and dependencies underlying nucleation under these conditions.

D. Complementary remarks

The application of a measuring kneader, microscopy, and the simple model of classical nucleation theory provide already deeper insight in the behavior of fondants during preparation. However, a number of points need to be discussed further.

Indeed, classical nucleation theory is strongly associated with equilibrium thermodynamics, whereas fondant production takes place far from equilibrium. Although theoretical treatments and computer simulations of classical nucleation under shear exist (see, for example,

Mura and Zaccone,³⁸ Richard and Speck,³⁹ and Goswami and Singh⁴²) these only approximate steady shear. They model the influence of steady shear as an increase in the energetic barrier of nucleation, and increase in the kinetic pre-factor of nucleation rate. However, because the proposed approximations are only valid for a constant shear rate, such models are not applicable to a system far from equilibrium where shear is heavily time and space dependent, as in the kneading machine in our experiments. Nevertheless in this study, the external time scales induced by kneading, $\tau_e \sim \mathcal{O}(1 \text{ s})$, are low compared to much larger typical molecular diffusion times^{34,43} (see Sec. IV C), which suggests a clear separation of time scales.

The contribution of Ostwald ripening to the crystal growth during the process remains an open question. These matters have been debated in the literature.⁴⁴ Whether released heat during crystallization possibly leads to dissolution of small crystals by locally increased temperature remains also open. It is suggested that crystal fragments smaller than about 1 μm probably dissolve again in agitated crystallizers (a) due to fluctuations in temperature and supersaturation and (b) because microcrystals might experience higher solubility than macrocrystals.^{21,33} To distinguish these possible processes from monotonic growth of small particles next to breakage of big particles during ongoing crystallization will be an interesting challenge.

A minor question is whether the temperature and kneading cause thermal decomposition of sucrose. It is well known that sucrose hydrolyzes to glucose and fructose under acidic conditions. For pH-values between 6 and 7, significant hydrolysis is unlikely and has been ignored here. Studying thermal degradation of sucrose in aqueous solutions via optical rotation, Eggleston⁴⁵ observed “very little sucrose degradation” for a solution containing 65% (w/w) sucrose heated to 100 °C for four hours (much longer than in the present study). Similarly, when heating pure sucrose at 10 °C min^{-1} , Lee *et al.*⁴⁶ found no decomposition compounds via HPLC analysis after 98.7 °C was reached, and only 0.365% glucose and 0.003% 5-HMF were detected at a target temperature of 150 °C (significantly higher than in the present study). With these references as comparison to our systems, this is considered not significant to the general trends and argumentation in this paper. Nevertheless, it might be of interest to study the precise effect of heating on possible decomposition and, subsequently, crystallization in such highly concentrated systems in future investigations.

V. CONCLUSION

In this study, we were able to shed more light on the process of crystallization out of highly supersaturated, agitated sucrose solutions. When looking at the temporal change in apparent viscosity of the dispersion as measured via torque of the kneading system, we argue that for the concentrations and temperatures used in this study, the counteracting effects of rise in crystal content and resulting decrease in solution concentration lead to a minimum in measured torque before final crystallization. For the observed peak in measured torque, microscopy images show that a high number of crystal conglomerates form during crystallization but are significantly reduced after further kneading, indicating fracture and breakup due to the applied shear forces and friction for high crystal content. The change in duration of this process depending on temperature and composition could be shown to follow classical nucleation theory models of

thermodynamics, with the peak time being dependent on temperature and supersaturation in the same way as predicted.

These findings help better understand the physics of the crystallization processes of sucrose under these highly non-equilibrium conditions, as they are present, for example, in the production of fondant in confectionery. They may, thus, help planning production processes and controlling crystallization properties in products of confectionery or pharmaceuticals, but mainly constitute a contribution to the physical understanding of empirically observed crystallization kinetics.

SUPPLEMENTARY MATERIAL

See the supplementary material for details on the preparation of sucrose solutions, images of light microscopy, and values of calculated torque peak times with respect to supersaturation.

ACKNOWLEDGMENTS

We wish to acknowledge the support of Südzucker AG (Mannheim, Germany) who provided the sucrose and measuring kneader used in the measurements. We thank the referees for their helpful and constructive criticism, which allowed improvement of the manuscript.

AUTHOR DECLARATIONS

Conflict of Interest

The authors have no conflicts to disclose.

Author Contributions

Hannah M. Hartge: Conceptualization (equal); Data curation (equal); Formal analysis (equal); Investigation (equal); Methodology (equal); Project administration (equal); Software (equal); Validation (equal); Visualization (equal); Writing – original draft (equal); Writing – review & editing (equal). **Eckhard Flöter:** Conceptualization (supporting); Supervision (supporting); Writing – review & editing (supporting). **Thomas A. Vilgis:** Conceptualization (equal); Methodology (equal); Project administration (equal); Resources (equal); Supervision (equal); Writing – review & editing (equal).

DATA AVAILABILITY

The data that support the findings of this study are available within the article and its supplementary material.

APPENDIX A: VISCOSITY OF DISPERSIONS

For highly concentrated, coarse poly-disperse systems, adequate theoretical models remain a difficult challenge due to the complex influences of particle shapes and sizes, particle deformability, packing density, hydrodynamics, and attractive and repulsive forces.^{26,47} Nonetheless, multiple empirical or semi-empirical models have been proposed like those by Krieger and Dougherty⁴⁸ or Toda and Furuse⁴⁹ (see also Tadros²⁶ or Coussot⁴⁷ for more details on different models). Krieger and Dougherty, for example, propose the following equation by making use of a mean field approximation:

$$\eta_r = \left(1 - \frac{\Phi}{\Phi_p}\right)^{[\eta]\Phi_p}, \quad (\text{A1})$$

where η_r is the relative viscosity, $[\eta]$ is the intrinsic viscosity, Φ is the volume fraction of particles in the dispersion, and Φ_p is the maximum packing fraction of particles.

In the limit of small Φ , this model approaches Einstein's classical equation for the viscosity of dilute, homogeneous dispersions with small spheres:^{50,51} $\eta_r = 1 + [\eta]\Phi$, with $[\eta] = 2.5$ for infinitely dispersed rigid spheres. While Einstein's equation is based in physical theory, its application is quite restricted and not useful for concentrated dispersions.

Models like the one of Dougherty and Krieger are supposed to cover the whole range of concentrations, but determining $[\eta]$ and Φ_p for a dispersion of irregularly shaped particles with a broad and, in this case, changing size distribution is difficult. Thus, it is not used for further studies in this work.

APPENDIX B: EMPIRICAL VALUES ON SOLUBILITY AND VISCOSITY

Values for equilibrium concentration of aqueous sucrose solutions are calculated by Eq. (5.14) from Bubnik and Kadlec,³⁰ which is identical to the equation given by the International Commission for Uniform Methods of Sugar Analysis ICUMSA in Specification SPS-2.²⁸ This is a heuristic equation fitted to empirical values of sucrose solubility,

$$c_{\text{sol}} = 64.447 + 0.08222T + 0.0016169T^2 - 0.000001558T^3 - 0.000000463T^4, \quad (\text{B1})$$

where c_{sol} is the solubility concentration in weight percent, and T is the temperature of the solution in °C. This equation is used purely for comparison with empirically measured values of sucrose solubility found in the literature and has no physical meaning.

Estimated viscosity of sucrose solutions is calculated by an expression fitted to empirical values of measured viscosities given by Genotelle,²⁹ as cited in Mathlouthi and Reiser,⁸ and similar values by ICUMSA,²⁸

$$\log \eta_r = 22.46x_{\text{suc}} - 0.114 + P(1.1 + 43.1x_{\text{suc}}^{1.25}), \quad (\text{B2})$$

with x_{suc} being the mole fraction of sucrose in the solution, and $P = (30^\circ\text{C} - T)/(91^\circ\text{C} + T)$, a temperature function valid for water. Again, remember this equation is used purely for comparison with empirical values found in the literature and is not used for physical explanations.

APPENDIX C: ACTIVITY COEFFICIENTS

For estimation of activity coefficients in order to calculate supersaturation, a modified molecular UNIQUAC model was used. This quasicheical model was successfully applied to sucrose and other sugars for a wide range of concentrations by Peres and Macedo;⁴¹ thus, their calculated parameters are adopted in this work, as also seen, for example, in Ouiazzane *et al.*¹² See Peres and Macedo⁴¹ for details and empirical constants.

In this model, the activity coefficient of sucrose γ is calculated as the sum of a combinatorial and a residual term,

$$\ln \gamma = \ln \gamma_c + \ln \gamma_r. \quad (C1)$$

The combinatorial term $\ln \gamma_c$ is given by

$$\ln \gamma_c = \ln(\varphi/x_s) + 1 - \varphi/x_s, \quad (C2)$$

with molar fraction of sucrose x_s , molar fraction of water x_w , and

$$\varphi = x_s r_s^{2/3} / \sum_{i=s,w} x_i r_i^{2/3}. \quad (C3)$$

Here, $i = s, w$ are the two system components sucrose and water, and molecular volume parameters $r_s = 14.5496$ for sucrose and $r_w = 0.92$ for water are used.

The residual term $\ln \gamma_r$ is given by

$$\ln \gamma_r = q_s \left[1 - \ln \left(\sum_i \Theta_i \tau_{is} \right) - \sum_i \frac{\Theta_i \tau_{si}}{\sum_j \Theta_j \tau_{ji}} \right], \quad (C4)$$

where the surface area fraction Θ_i of component i is calculated as

$$\Theta_i = x_i q_i / \sum_j x_j q_j, \quad (C5)$$

and surface parameters are $q_s = 13.764$ for sucrose and $q_w = 1.4$ for water.

The Boltzmann factors τ_{ij} are given as

$$\tau_{ij} = \exp(-a_{ij}/T_K), \quad (C6)$$

with T_K being temperature in Kelvin, and a_{ij} being linearly temperature-dependent interaction parameters of the sucrose–water system given as

$$a_{sw} = -89.3391 + 0.3280(T_K - 298.15), \quad (C7)$$

$$a_{ws} = 118.9952 - 0.3410(T_K - 298.15), \quad (C8)$$

$$a_{ss} = a_{ww} = 0. \quad (C9)$$

REFERENCES

- ¹R. Lees, *Factors Affecting Crystallization in Boiled Sweets, Fondants and Other Confectionery*, Scientific and Technical Surveys No. 42 (The British Food Manufacturing Industries Research Association, Leatherhead, Surrey, 1965).
- ²R. W. Hartel, *Crystallization in Foods* (Aspen Publishers, Inc., Gaithersburg, Maryland, 2001).
- ³C. A. Beevers, T. R. R. McDonald, J. H. Robertson, and F. Stern, "The crystal structure of sucrose," *Acta Crystallogr.* **5**, 689–690 (1952).
- ⁴A. VanHook, "Habit modification of sucrose crystals: A lecture," *J. Am. Soc. Sugar Beet Technol.* **22**(1), 60–72 (1983).
- ⁵G. Mantovani, G. Vaccari, C. A. Accorsi, D. Aquilano, and M. Rubbo, "Twin growth of sucrose crystals," *J. Cryst. Growth* **62**, 595–602 (1983).
- ⁶D. Aquilano, M. Rubbo, G. Mantovani, G. Sgualdino, and G. Vaccari, "Equilibrium and growth forms of sucrose crystals in the {h0l} zone: I. Theoretical treatment of {101}-d form," *J. Cryst. Growth* **74**, 10–20 (1986).
- ⁷D. Aquilano, M. Rubbo, G. Mantovani, G. Sgualdino, and G. Vaccari, "Equilibrium and growth forms of sucrose crystals in the {h0l} zone: II. Growth kinetics of the {101}-d form," *J. Cryst. Growth* **83**, 77–83 (1987).
- ⁸*Sucrose: Properties and Applications*, edited by M. Mathlouthi and P. Reiser (Springer US, Boston, MA, 1995).
- ⁹C. J. Kedward, W. MacNaughtan, J. M. V. Blanshard, and J. R. Mitchell, "Crystallization kinetics of lactose and sucrose based on isothermal differential scanning calorimetry," *J. Food Sci.* **63**, 192–197 (2008).
- ¹⁰M. Mathlouthi and J. Genotelle, "Role of water in sucrose crystallization," *Carbohydr. Polym.* **37**, 335–342 (1998).
- ¹¹C. J. Kedward, W. MacNaughtan, and J. R. Mitchell, "Isothermal and non-isothermal crystallization in amorphous sucrose and lactose at low moisture contents," *Carbohydr. Res.* **329**, 423–430 (2000).
- ¹²S. Ouiazzane, B. Messnaoui, S. Abderafi, J. Wouters, and T. Bounahmidi, "Estimation of sucrose crystallization kinetics from batch crystallizer data," *J. Cryst. Growth* **310**, 798–803 (2008).
- ¹³I. A. Khaddour, L. S. Bento, A. M. Ferreira, and F. A. Rocha, "Kinetics and thermodynamics of sucrose crystallization from pure solution at different initial supersaturations," *Surf. Sci.* **604**, 1208–1214 (2010).
- ¹⁴K. Vasanth Kumar, P. Martins, and F. Rocha, "Modelling of the batch sucrose crystallization kinetics using artificial neural networks: Comparison with conventional regression analysis," *Ind. Eng. Chem. Res.* **47**, 4917–4923 (2008).
- ¹⁵P. Quintana-Hernández, E. Bolaños-Reynoso, B. Miranda-Castro, and L. Salcedo-Estrada, "Mathematical modeling and kinetic parameter estimation in batch crystallization," *AIChE J.* **50**(7), 1407–1417 (2004).
- ¹⁶R. W. Hartel, R. Ergun, and S. Vogel, "Phase/state transitions of confectionery sweeteners: Thermodynamic and kinetic aspects," *Compr. Rev. Food Sci. Food Safety* **10**, 17–32 (2011).
- ¹⁷R. W. Hartel, J. H. von Elbe, and R. Hofberger, *Confectionery Science and Technology* (Springer International Publishing, Cham, 2018).
- ¹⁸O. Ozcan, R. M. Yildirim, O. S. Toker, N. Akbas, G. Ozulku, and M. Yaman, "The effect of invertase concentration on quality parameters of fondant," *J. Food Sci. Technol.* **56**, 4242–4250 (2019).
- ¹⁹J. McGill and R. W. Hartel, "Water relations in confections," in *Water Activity in Foods*, 1st ed., edited by G. V. Barbosa-Cánovas, A. J. Fontana, S. J. Schmidt, and T. P. Labuza (Wiley, 2020), pp. 483–500.
- ²⁰G. Vaccari and G. Mantovani, "Sucrose crystallization," in *Sucrose: Properties and Applications*, edited by M. Mathlouthi and P. Reiser (Springer US, Boston, MA, 1995), pp. 33–74.
- ²¹J. W. Mullin, *Crystallization*, 4th ed. (Butterworth-Heinemann, Oxford, 2001).
- ²²I. V. Markov, "Nucleation at surfaces," in *Springer Handbook of Crystal Growth*, edited by G. Dhanaraj, K. Byrappa, V. Prasad, and M. Dudley (Springer, Heidelberg/New York, 2010), pp. 17–52.
- ²³T. L. Threlfall and S. J. Coles, "A perspective on the growth-only zone, the secondary nucleation threshold and crystal size distribution in solution crystallization," *CrystEngComm* **18**, 369–378 (2016).
- ²⁴J. J. De Yoreo and P. G. Vekilov, "Principles of crystal nucleation and growth," in *Biomaterialization*, edited by Patricia M. Dove, James J. De Yoreo, and S. Weiner (De Gruyter, Berlin/Boston, 2018), pp. 57–94.
- ²⁵D. Zheng, W. Zou, J. Yan, C. Peng, Y. Fu, B. Li, L. Zeng, T. Huang, and F. Zhang, "Coupling of contact nucleation kinetics with breakage model for crystallization of sodium chloride crystal in fluidized bed crystallizer," *J. Chem.* **2019**, e2150560.
- ²⁶T. F. Tadros, *Rheology of Dispersions: Principles and Applications* (Wiley-VCH Verlag GmbH & Co. KGaA, Weinheim, Germany, 2010).
- ²⁷M. Quintas, T. R. S. Brandão, C. L. M. Silva, and R. L. Cunha, "Rheology of supersaturated sucrose solutions," *J. Food Eng.* **77**, 844–852 (2006).
- ²⁸The International Commission for Uniform Methods of Sugar Analysis (ICUMSA), *ICUMSA Methods Book 2019* (Dr. Albert Bartens KG, Berlin, Germany, 2019).
- ²⁹J. Genotelle, "Expression de la viscosité des solutions sucrées," *Industries Alimentaires Agricoles* **95**, 747–755 (1978).
- ³⁰Z. Bubnik and P. Kadlec, "Sucrose solubility," in *Sucrose: Properties and Applications*, edited by M. Mathlouthi and P. Reiser (Springer US, Boston, MA, 1995), pp. 101–125.
- ³¹A. V. Shastry, "Batch crystallization of sucrose from high concentration syrups," M.S. thesis (University of Wisconsin, Madison, WI, 1991).
- ³²A. Chernov, N. Zaitseva, and L. Rashkovich, "Secondary nucleation induced by the cracking of a growing crystal: KH_2PO_4 (KDP) and $\text{K}(\text{H}_2\text{D})_2\text{PO}_4$ (DKDP)," *J. Cryst. Growth* **102**, 793–800 (1990).
- ³³H. Garabedian and R. F. Strickland-Constable, "Collision breeding of crystal nuclei: Sodium chlorate. I," *J. Cryst. Growth* **13–14**, 506–509 (1972).
- ³⁴H. C. Price, J. Mattsson, and B. J. Murray, "Sucrose diffusion in aqueous solution," *Phys. Chem. Chem. Phys.* **18**, 19207–19216 (2016).

- ³⁵D. Levenson and R. Hartel, "Nucleation of amorphous sucrose-corn syrup mixtures," *J. Food Eng.* **69**, 9–15 (2005).
- ³⁶D. Champion, H. Hervet, G. Blond, M. Le Meste, and D. Simatos, "Translational diffusion in sucrose solutions in the vicinity of their glass transition temperature," *J. Phys. Chem. B* **101**, 10674–10679 (1997).
- ³⁷Y. Roos, "Melting and glass transitions of low molecular weight carbohydrates," *Carbohydr. Res.* **238**, 39–48 (1993).
- ³⁸F. Mura and A. Zaccone, "Effects of shear flow on phase nucleation and crystallization," *Phys. Rev. E* **93**, 042803 (2016).
- ³⁹D. Richard and T. Speck, "Classical nucleation theory for the crystallization kinetics in sheared liquids," *Phys. Rev. E* **99**, 062801 (2019).
- ⁴⁰J. M. Schall, G. Capellades, and A. S. Myerson, "Methods for estimating supersaturation in antisolvent crystallization systems," *CrystEngComm* **21**, 5811–5817 (2019).
- ⁴¹A. M. Peres and E. A. Macedo, "Thermodynamic properties of sugars in aqueous solutions: Correlation and prediction using a modified UNIQUAC model," *Fluid Phase Equilib.* **123**, 71–95 (1996).
- ⁴²A. Goswami and J. K. Singh, "Homogeneous nucleation of sheared liquids: Advances and insights from simulations and theory," *Phys. Chem. Chem. Phys.* **23**, 15402–15419 (2021).
- ⁴³N. Ekdawi-Sever, J. J. de Pablo, E. Feick, and E. von Meerwall, "Diffusion of sucrose and α , α -trehalose in aqueous solutions," *J. Phys. Chem. A* **107**, 936–943 (2003).
- ⁴⁴J. Blanshard, A. Muhr, and A. Gough, "Crystallization from concentrated sucrose solutions," *Water Relationships in Foods: Advances in the 1980s and Trends for the 1990s* (Springer, Boston, 1991), pp. 639–655.
- ⁴⁵G. Eggleston, B. J. Trask-Morrell, and J. R. Vercellotti, "Use of differential scanning calorimetry and thermogravimetric analysis to characterize the thermal degradation of crystalline sucrose and dried sucrose-salt residues," *J. Agric. Food Chem.* **44**, 3319–3325 (1996).
- ⁴⁶J. W. Lee, L. C. Thomas, J. Jerrell, H. Feng, K. R. Cadwallader, and S. J. Schmidt, "Investigation of thermal decomposition as the kinetic process that causes the loss of crystalline structure in sucrose using a chemical analysis approach (Part II)," *J. Agric. Food Chem.* **59**, 702–712 (2011).
- ⁴⁷P. Coussot, *Mudflow Rheology and Dynamics*, IAHR/AIRH Monograph Series (A.A. Balkema, Rotterdam, 1997).
- ⁴⁸I. M. Krieger and T. J. Dougherty, "A Mechanism for Non-Newtonian flow in suspensions of rigid spheres," *Trans. Soc. Rheol.* **3**, 137–152 (1959).
- ⁴⁹K. Toda and H. Furuse, "Extension of Einstein's viscosity equation to that for concentrated dispersions of solutes and particles," *J. Biosci. Bioeng.* **102**, 524–528 (2006).
- ⁵⁰A. Einstein, "Eine neue Bestimmung der Moleküldimensionen," *Ann. Phys.* **324**, 289–306 (1906).
- ⁵¹A. Einstein, "Berichtigung zu meiner Arbeit: Eine neue Bestimmung der Moleküldimensionen," *Ann. Phys.* **339**, 591–592 (1911).